The effect of creep in the interaction between TBM, lining and rock

Scientific Report – Period 01.04.2015 – 31.03.2018

Report

Author(s):
Anagnostou, Georgios ⓘD

Scientific Report – Period 01.04.2015 – 31.03.2018

Main applicant	Anagnostou, Georgios
Project title	The effect of creep in the interaction between TBM, lining and rock

1 Progress of the works

1.1 Overview

The project works are, as explained in the proposal, subdivided in six stages. The report presents in the following sections the progress done for each of these six stages.

1.2 Constitutive model formulation, implementation and validation in the framework of one-step solution

The following constitutive models were evaluated due to their adequacy for the purpose of the present project: Perzyna MC, SHELVIP, 3SC and CVISC. The last two were included during the progress of the work, since they have been used for the analysis of creep effects in tunnelling by other researchers in recent time. A brief explanation of all constitutive models is given in Appendix 1.

In a first step, the four constitutive models mentioned above were implemented and validated for a tunnel excavation application based upon a step-by-step simulation of tunnel advance. The implementation was done in form of a subroutine UMAT (User defined MATerial model in ABAQUS) into the commercial finite element (FE) program ABAQUS [1]. The implementation in ABAQUS allows generating benchmarks to verify results to be obtained with a one-step solution with the FE code HYDMEC, which was developed in our group [2]. The one-step solution solves the problem of the advancing head in one step and is therefore more efficient than the step-by-step solution method which approaches the steady state asymptotically by simulating several excavation steps. Thus the use of HYDMEC will allow performing parametric analysis in a reasonable time.

The Perzyna MC, 3SC and CVISC constitutive model were successfully implemented in ABAQUS and validated; whereas the implementation of SHELVIP constitutive model is currently on-going. Afterwards the implementation in HYDMEC will follow. Until now the situation considered for the simulations corresponds to a deep cylindrical tunnel in a homogeneous and isotropic ground under an isotropic initial stress field, excavated with a shield TBM. Thus simulations were performed for an axial symmetric model. The geotechnical parameters correspond to fault material (*cf.* Table 1 in Appendix 2). The tunnel support consists of segmental lining where the annulus created by the overcut is grouted immediately after positioning of the segments.

1.3 Calibration of the parameters of the constitutive model through experiments and results of field measurements

Calibration of the aforementioned constitutive models has to be performed through laboratory tests and verification with field measurements of current project works. Within the frame of research works on mechanical behaviour of fault material a new triaxial cell was designed and constructed. The cell allows running tests controlling pore pressure at both ends of the specimen and also for measuring deformation (axial and radial) close to the specimen, *i.e.* in the cell. The cell supports high confining pressures up to 250 bar. An innovation of the testing system is the improvement of the membrane in order to allow measuring pore pressure at the middle of the specimen and thus being able to avoid generation of excess pore pressure. A special water pipeline was developed, which is flexible to follow deformations of the specimen and stiff to support cell pressure without influencing the measurement of the water pressure in the pipeline. Furthermore, the temperature of the cell and the cell-pressure amplifier is kept constant with a specially developed closed circular pipeline. The tightness of the modified membrane was tested successfully. The first so called "pure creep test" (*i.e.* eliminating effects due to excess pore pressure) on a fully saturated Kakirite specimen from the planned second tube of the Gotthard motorway tunnel is on-going. The elasto-plastic parameters of this material are known, since we ran previously an extensive testing program consisting of 21 triaxial tests measuring pore water pressure. The tested material stems from the formations Mesozoic, Permocarbon and Guspis Zone. We have several remaining samples from this testing campaign. A second triaxial cell is ready so that tests with two equipments can be run simultaneously after finishing the first test. The results will allow to evaluate the adequacy of the different constitutive models to describe material behaviour under pure creep conditions and the calibration of their respective parameters.

The evaluation of the convergence and extensometer measurements in the carbon and autochthon section of the Loetschberg Basetunnel is currently on-going. The selected sections exhibited during excavation and since commissioning in 2007 a pronounced time-dependent behaviour. Non-uniformly distributed deformations on the tunnel cross section could be correlated to the orientation of schistosity plane and lithological variation but without taking into account time dependent effects as consolidation or creep [3].

The adequacy of the model to predict deformations in other projects and applications will be proofed in terms of evaluating the capability of the model to reproduce the time dependent deformations measured in-situ. This will be done with the most adequate model selected on the base of the pure creep test results and with the respective calibration of the parameters considering detailed geological and geotechnical information.

1.4 Thrust force and lining pressure calculations

The aim of this stage is to analyse numerically the influence of creep on TBM tunnelling. More specifically, we investigate two of the most important hazard scenarios in TBM tunnelling - shield jamming and overstressing of the lining.

Due to the lack of knowledge concerning pure creep behaviour (no experimental results or field measurements certainly without containing consolidation effects were available) the parametric analyses were run considering models as simple as possible, *i.e.* containing only one viscosity and one St. Venant element. The analyses with more sophisticated models like SHELVIP, 3SC and general CVISC (*i.e.* with two viscosity elements) is, due to the lack of knowledge mentioned before, not justifiable at the present stage of the project and the additional complexity introduced by considering more aspects will make interpretation of the parametric analyses much

more difficult. The goal of the present parametric analysis is to evaluate qualitatively the hazard scenarios mentioned above (*i.e.* shield jamming and overstressing of the lining). It becomes evident that results will depend besides the considered viscosity parameters also on the coupling of the viscosity elements with the other fundamental rheological models, *i.e.* in a Bingham's, Kelvin's or Maxwell's model. Thus, simulations were performed with the Perzyna MC model, which contains a Bingham's model and two simplified CVISC models. For the present analyses the CVISC model was simplified by neglecting the deformation contribution of the viscosity parameter of either the Maxwell's model (*i.e.* considering an infinite viscosity of this element) or of the Kelvin's model. The simplified CVISC models are referred hereinafter as CVISC (Kelvin) and CVISC (Maxwell) respectively. The range of the viscosity parameters chosen for the three parametric analyses (Perzyna MC and the two simplified CVISC models) covers the expected range for squeezing rock (*cf.* [4-8]).

In Appendix 2 the parameters considered are listed and the results of the parametric analyses are commented and summarized in diagrams. The main findings of these parametric analyses are:

- The most relevant case with respect to the two hazard scenarios mentioned above is the situation during TBM standstills.
- The risk of the two hazard scenarios depends strongly on the constitutive model considered and is (ordered from lower to higher risk) lower with Perzyna MC than with CVISC (Kelvin) and CVISC (Maxwell) model.
- From beginning of a standstill, the required thrust force for restarting excavation remains approximately constant until a critical time-point t_{crit}. Afterwards the required thrust force increases. Thus, t_{crit} denotes the maximal standstill time within no additional thrust force for restarting, as during excavation, is required. Thus, for standstill time shorter than t_{crit} certainly no jamming risk exists. The critical time depends on the product of TBM advance rate v and viscosity η. In good approximation the analysed geotechnical situation the dependency of t_{crit} on the product $\eta\ v$ can be described independently of the chosen constitutive model with a simple function (*cf.* Appendix 2).
- For the geotechnical situation investigated and assuming Perzyna's MC model, the thrust force that is required to resume TBM advance is lower than the typically installed thrust forces even if considering a very long standstill time. The CVISC (Kelvin) constitutive model results in the case of long standstills to a thrust force, which may be twice as high as typically installed thrust forces. The behaviour of the CVISC (Maxwell) model is even more unfavourable: the required thrust force is up to three times higher than typically installed thrust forces even in the case of relatively short standstills and low viscosity (very high shield jamming risk).
- The risk of overstressing of the tunnel lining for the geotechnical situation investigated is similar as for shield jamming. With a Perzyna MC model the calculated pressure corresponds approximately to the typical value of lining strength. With CVISC model the calculated pressure exceeds the lining strength by factor two and three for CVISC (Kelvin) and CVISC (Maxwell) models respectively making tunnelling in ground with the model's behaviour extremely problematic if not impossible.

After the completion of stage 1 and 2 (*cf.* Section 1.2 and Section 1.3) and selection of the most appropriate constitutive model for squeezing ground prone to creep a systematic parametric analyses will be performed in order to prepare design nomograms for quantifying the required thrust force and the ground pressures developing on the lining in squeezing ground.

1.5 Effect of time dependency of backfilling material

This stage will be investigated after the completion of stages 1, 2, 3 and 6.

1.6 Comparative evaluation of lining systems under creep conditions

The two basic lining types in ground prone to squeeze are designed obeying either the so-called resistance principle or the so-called yielding principle. The aim of this stage is to compare critically the behaviour under creep conditions of these two basic lining types. This issue was investigated in our group but without considering any time effects [9-10]. For the present analyses time-dependent effects in the ground (creep) as well as in the backfilling material should be taken into account as for example the model CEB MC90-99 (approved by ACI Committee [11]). The numerical simulations will be performed with the same assumptions as in stage 3 (*cf.* Section 1.4).

This stage will be investigated after the completion of stages 1, 2, 3 and 6.

1.7 Comparison and combination of consolidation and creep mechanisms

The aim of this stage is to determine under which conditions and for which material properties which mechanism of time dependency (creep and or consolidation) is dominant for the ground response.

We investigated numerically similarities and differences in the behaviour of a ground either prone to creep or to consolidate. More precisely ground pressures developing on the shield of a TBM during excavation and standstill, the required thrust force to restart tunnelling, the pressure on the lining and the extrusion deformations and stability of the tunnel face are analysed. In a first series of simulations two cases are considered with each only one time dependent mechanism active, namely a dry ground prone to creep and a saturated ground prone to consolidate but without containing viscosity. Furthermore for the consolidation case a uniform initial hydraulic head field and atmospheric pore pressures at the excavation boundary is assumed. An overview of the additional geotechnical parameters for a ground prone to consolidate is given in Table 4 of Appendix 3. For a ground prone to creep Perzyna MC constitutive model was considered due to its simplicity (it contains only one viscosity parameter). This allows a simpler comparison of the ground behaviour for the creep case with the consolidation case. Time effects depend on the respective geotechnical parameters but also on the advance rate v. Depending on the case analysed results are governed according to different relations between these parameters, *i.e.* for creep the product of advance rate with the viscosity $\eta\,v$ [12] while for consolidation the ratio of advance rate with the permeability v/k [13] must be considered. It must be pointed out that the product $\eta\,v$ is not dimensionless as it is the ratio v/k. In the present study these parameter relations were varied for both cases within the same ranges.

In Appendix 3 the parameters considered are listed and the results of the parametric analyses are commented and summarized in diagrams. The comparison between the results corresponding to both cases, *i.e.* creep and consolidation concerning the shape of the curve, their absolute values and the variability of the parameters show:

-   Big similarity of the distribution of the normal pressure on the shield and on the lining (*cf.* Figs. 7a and 7b in Appendix 3)
-   Good similarity of the required thrust force for a restart after standstill (*cf.* Fig. 8a and 8b in Appendix 3)
-   Good to fair similarity of the pressure on the lining (*cf.* Fig. 9a and 9b in Appendix 3)

- Big similarity of the extrusion of the tunnel face during standstill (*cf.* Fig. 10a and 10b in Appendix 3).

Thus, time effects due to creep with a Perzyna MC model can be described similar as a consolidation case, *i.e.* for $\eta\,\nu < 10^4$ and $\eta\,\nu > 10^{11}$ no time effects can be observed. In the first case the viscosity is so low that it cannot storage enough stress to be released later , while in the other case the time for stress release exceeds the life-time of the tunnel. These cases are comparable with $\nu/k \leq 10^7$ and $\nu/k \geq 10^{14}$ where the high permeability lead to full drained conditions in advance and the extreme low permeability did not allow significant pore pressure dissipation during the life-time of the tunnel respectively (permanent undrained situation). Consequently the relevant range of viscosity when considering time effects with a Perzyna MC model is $10^4 < \eta\,\nu < 10^{11}$.

Depending on the evaluation of the pure creep laboratory tests the parametric study with Perzyna MC model will be extended or repeated with a more adequate constitutive model. Finally the combined case of creep and consolidation will be investigated in order to determine their different weighting on the time-dependent deformations for tunnelling with TBM.

2 Contributions of the SNF collaborator

The works carried out by the SNF-supported Ph.D. student Mr. Thomas Leone during the three years of the research project are listed below:

First year:

1. Implementation and validation of the step-by-step solution considering an unlined tunnel in a dry creeping ground.
2. Formulation of Perzyna's MC constitutive model in the framework of a step-by-step and one-step solution.
3. Implementation and validation of MC and Perzyna's MC constitutive models in the framework of a step-by-step solution.
4. Analytical formulation and evaluation of the strains and stresses of a cylindrical specimen subjected to triaxial load conditions considering Perzyna's MC, CVISC, 3SC and SHELVIP constitutive models.

Second year:

1. Implementation and validation of the step-by-step solution considering a lined tunnel excavated conventionally and excavated by a TBM both in dry creeping ground.
2. Formulation of CVISC and 3SC constitutive models in the framework of a step-by-step and one-step solution.
3. Implementation and validation of CVISC and 3SC constitutive models in the framework of a step-by-step solution.
4. Parametric analyses of the required thrust force and lining pressure considering Perzyna's MC constitutive model in the framework of a step-by-step solution.
5. Analytical formulation and evaluation of the displacements and stresses for a circular tunnel problem under plane strain conditions and isotropic loading considering a CVISC constitutive model.

Third year:

1. Implementation and validation of the step-by-step solution considering a lined tunnel excavated by a TBM in water saturated consolidating ground.
2. Parametric analyses of the required thrust force and lining pressure, considering CVISC and 3SC constitutive models in the framework of a step-by-step solution.
3. Comparison of the two time-dependent mechanisms consolidation and creep (considering MC constitutive model for consolidation mechanism and Perznya's MC constitutive model for creep mechanism) through thrust force, lining pressure and face extrusion calculations, results evaluation in the framework of a step-by-step solution.

The participation and submission of a conference paper with the title "TBM shield jamming and overstressing of the lining due to creep" to the WTC Tunnel Congress 2019 in Naples is planned. The abstract was accepted and the paper is in preparation and will be submitted in September 2018.

In the scientific future the SNF-supported Ph.D. student Mr. Thomas Leone will continue with the elaboration of the following tasks:

1. Formulation of SHELVIP constitutive model in the framework of a step-by-step and one-step solution.
2. Implementation and validation of SHELVIP constitutive model in the framework of a step-by-step solution.

3. Parametric analyses of the required thrust force and lining pressure considering SHELVIP constitutive model in the framework of a step-by-step solution.
4. Calibration of the parameters of the constitutive models based on the experimental results and evaluation of their suitability for modelling creep of fault materials.
5. Implementation and validation of the most suitable models in the framework of a one-step solution.
6. Verification of the calibrated selected models through field measurements.
7. Preparation of design aids (*e.g.* nomograms) to assess the risk of shield jamming and overstress of the lining in squeezing ground for the most suitable constitutive models.
8. Investigation of the effect of time dependency of backfilling materials.
9. Comparative evaluation of lining systems under creep conditions.
10. Simulations considering simultaneously both time-dependent mechanisms creep and consolidation in the framework of a step-by-step solution.

3 References

[1]   Dassault Systèmes (2012). Abaqus 6.12, Theory and Analysis User's Manual.

[2]   Anagnostou, G. (2007). Continuous tunnel excavation in a poro-elastoplastic medium. In: Tenth International Symposium on Numerical Models in Geomechanics, NUMOG X, Rhodes. Taylor & Francis Group, London, pp 183–188.

[3]   Mezger, F., Anagnostou, G. (2017). On the variability of squeezing in the carbon section of the Lötschberg Base Tunnel (internal report).

[4]   Cantieni, L., & Anagnostou, G. (2011). On a Paradox of Elasto-Plastic Tunnel Analysis. Rock Mechanics and Rock Engineering, 44(2), 129-147.

[5]   Pellet, F. (2009). Contact between a Tunnel Lining and a Damage-Susceptible Viscoplastic Medium. Computer Modeling in Engineering and Sciences, 52, 279-296.

[6]   Barla, G., Bonini, M., Debernardi, D. (2008). Time Dependent Deformations in Squeezing Tunnels. The 12th International Conference of IACMAG.

[7]   Bonini, M., Debernardi, D., Barla, M., & Barla, G. (2007). The Mechanical Behaviour of Clay Shales and Implications on the Design of Tunnels. Rock Mechanics and Rock Engineering, 42(2), 361.

[8]   Han-Ping Chin, J., Rogers, J.D. (1987): Creep parameters of rocks on an engineering scale, Rock Mechanics and Rock Engineering, vol 20: 137-146.

[9]   Mezger, F., Ramoni, M., Anagnostou, G., Dimitrakopoulos, A., & Meystre, N. (2017). Evaluation of higher capacity segmental lining systems when tunnelling in squeezing rock. Tunnelling and Underground Space Technology, 65, 200-214.

[10]   Mezger, F., Ramoni, M., & Anagnostou, G. (2018). Options for deformable segmental lining systems for tunnelling in squeezing rock. Tunnelling and Underground Space Technology, 76, 64-75.

[11]   ACI Committee 209 Report (2008). Guide for Modelling and Calculating Shrinkage and Creep in Hardened Concrete, ACI 209.2R-08.

[12]   Bernaud, D. (1991). Tunnels profonds dans les milieux viscoplastiques : approches expérimentale et numérique. Ecole Nationale des Ponts et Chaussées. Retrieved from https://pastel.archives-ouvertes.fr/tel-00529719

[13]   Anagnostou, G. 2008. The effect of tunnel advance rate on the surface settlements. In: Proc. 12th IACMAG, 579–586, Goa.

[14]   Pimentel, E., Dong, W. & Anagnostou, G. (2011). Ceneri Base Tunnel – AlpTransit project L841-01, Laboratory triaxial tests on rock material, Report Nr. 1 (Samples SIG_1720, SIG_1603, SIG_1680 and Gbc-SE-1088-R-Nr.1), Report Nr. 112701. Zurich, Switzerland: IGT, ETH Zurich.

[15]   Pimentel, E., Dong, W. & Anagnostou, G. (2012). Gibraltar strait fixed link – Tunnel project, Experimental investigations on the strength and deformability of the Breccias, Report Nr. 121309. Zurich, Switzerland: IGT, ETH Zurich.

[16]   Pimentel, E. & Anagnostou, G. (2014). Verzweigungskaverne I – Tunnel Visp, Felsmechanische Laborversuche, Bericht Nr. 143001. Zurich, Switzerland: IGT, ETH Zurich (in German).

[17]   Pimentel, E., Dong, W. & Anagnostou, G. (2014). Semmering Basistunnel, Felsmechanische Laborversuche, Schlussbericht, Bericht Nr. 143002. Zurich, Switzerland: IGT, ETH Zurich (in German).

[18]   Pimentel, E. & Anagnostou, G. (2017). Karawanks Tunnel, triaxial tests – final report, Report No. 164305. Zurich, Switzerland: IGT, ETH Zurich.

[19]   Pimentel, E. & Anagnostou, G. (2017). N2 Gotthard-Strassentunnel: Zweite Tunnelröhre, Felsmechanische Triaxialversuche -Schlussbericht, Report No. 174222. Zurich, Switzerland: IGT, ETH Zurich (in German).

[20]   Barla, G., Debernardi, D., & Sterpi, D. (2012). Time-Dependent Modeling of Tunnels in Squeezing Conditions. International Journal of Geomechanics, 12(6), 697-710.

[21]   ITASCA (2011). FLAC Creep Material Models. ITASCA Consulting Group Inc., Minneapolis.

[22]   Puzrin, A. (2012). Constitutive Modelling in Geomechanics. Springer Verlag.

[23]   Cailletaud, G. (2012). Mécanique des matériaux solides, Notes de cures, MINES Paristech, Paris, France (in French).

[24]   Burgers, J. M. (1935). Mechanical considerations, model systems, phenomenological theories of relaxation and of viscosity. In First report on viscosity and plasticity. New York, NY, USA: Nordemann Publishing Company.

[25]   Clausen, J., Damkilde, L., & Andersen, L. (2007). An efficient return algorithm for non-associated plasticity with linear yield criteria in principal stress space. Computers & Structures, 85(23), 1795-1807.

[26]   Simo, J. C., & Taylor, R. L. (1985). Consistent tangent operators for rate-independent elastoplasticity. Computer Methods in Applied Mechanics and Engineering, 48(1), 101-118.

[27]   Perzyna, P. (1966). Fundamental Problems in Viscoplasticity. 9, 243-377.

[28]   FLAC update nr. 440, "fixed a bug in Burgers-creep viscoplastic model" (2017). https://www.itascacg.com/software/flac/updates/flac-80-64-bit, [Accessed 26 March 2018].

[29]   Herrenknecht, M., Bäppler, K., Burger, W., 2010. Tunnelling through squeezing rock with TBM. In: Brenner Base Tunnel and Access Routes, Brenner Congress, Innsbruck.

Ernst & Sohn Verlag für Architektur und technische Wissenschaften GmbH Berlin, pp. 45–54.

[30] Ramoni, M., Lavdas, N., & Anagnostou, G. (2011). Squeezing loading of segmental linings and the effect of backfilling. Tunnelling and Underground Space Technology, 26(6), 692-717.

[31] Sänger, B., 2006. Disc cutters for hardrock TBM 1986–2006 – history and tendencies of development. Felsbau 24 (6), 46–51.

[32] Vigl, L., Gütter, W., Häger, M., 1999. Doppelschild-TBM – Stand der Technik und Perspektiven. Felsbau 17 (5), 475–485.

[33] Ramoni, M. (2010). On the feasibility of TBM drives in squeezing ground and the risk of shield jamming. (236), ETH. Retrieved from http://hdl.handle.net/20.500.11850/30138

Appendix 1

In this Appendix a brief explanation of the selected constitutive models is given.

Perzyna MC and SHELVIP constitutive model were extensively explained in the proposal. Through back analysis of a cross section of the Saint Martin La Porte access tunnel of the Lyon-Turin base tunnel, it was shown that the 3SC and the SHELVIP constitutive model reproduce very well the deformations observed during tunnel excavation due to squeezing [20] and thus the 3SC constitutive model was also considered as adequate model for the present project. A simplified version of this constitutive model will be firstly used, which neglects the gradual mechanical damage of rock (and therefore avoiding additional complexity for first comparisons with other constitutive models). The CVISC constitutive model is implemented into the commercial finite difference program FLAC [21] and thus widely used, also due to good fitting between simulation results and in situ field measurements in tunnel projects (*i.e.* in the St. Martin La Porte access tunnel [5, 6] and Raticosa tunnel [7]).

The strains of the aforementioned constitutive models can be idealised through a combination in series and/or in parallel of the following fundamental rheological models: spring for modelling the elasticity (Hooke's model), piston for the linear viscosity (Newton's model) and plastic slider for the perfect plastic behaviour (St. Venant's model). The coupling of a spring and a piston in series is known as Maxwell's model [22], while its coupling in parallel represents Kelvin's model [22]. Another known composed rheological model is Bingham's model, which is constructed by coupling a plastic slider and a piston in parallel. A generalized form of this model is known as the generalized Bingham's model [23], which is constructed by coupling a plastic slider, a spring and a piston in parallel. Moreover, the coupling in series of Kelvin's and Maxwell's model is called Burger's model [24]. Thus, for a pure creep test (*i.e.* under constant deviatoric stress) the deformations produced by: a) Kelvin's model are viscoelastic and reversible (*i.e.* when the specimen is unloaded the deformations recover completely); b) Maxwell's model are viscoelastic and irreversible (*i.e.* when the specimen is unloaded the deformations will not recover completely as in the case of a plastic model); c) Bingham's model are viscoplastic.

The total strain of Perzyna MC constitutive model is idealised through the coupling in series of Hooke's and Bingham's model (*cf.* Fig. 1 (a)), while for the SHELVIP constitutive model it is done by Hooke's, St. Venant's and the generalized Bingham's model coupled in series (*cf.* Fig. 1 (b)). For the 3SC (*cf.* Fig. 1 (c)) and CVISC constitutive model (*cf.* Fig. 1 (d)) the total strain is subdivided into a deviatoric and volumetric strain (which are defined as the total strain in form of a tensor of second order). The deviatoric strain is modelled through: Hooke's, Kelvin's and Bingham's model coupled in series for the 3SC constitutive model; Burger's and St. Venant's model coupled in series for the CVISC constitutive model. The volumetric strain of the 3SC and CVISC constitutive model are modelled through Hooke's and St. Venant's model coupled in series. In FLAC's manual the CVISC constitutive model is also called "Burgers-creep viscoplastic model" which is misleading since it simulates only viscoelastic behaviour.

All the four constitutive models mentioned above contain a plastic component (St. Venant model), which is defined in form of a failure criterion. The Perzyna MC, 3SC and CVISC constitutive model consider Mohr-Coulomb (MC) failure criterion. Whereas, SHELVIP constitutive model considers Drucker-Prager (DP) failure criterion. ABAQUS does not allow combining a UMAT with a built-in subroutine, *i.e.* the ABAQUS built-in subroutine of MC failure criterion cannot be used. Thus, the MC failure criterion was implemented after Clausen et al. [25]. The Clausen procedure was chosen because quadratic convergence rate of the iterative method is achieved, by mathematical derivation of a stiffness matrix compatible with Newton-Raphson

method, so called consistent stiffness matrix [26]. The consistent stiffness matrix is not suited for Perzyna MC, 3SC and SHELVIP model, because they consider the overstress theory of Perzyna [27]. Therefore, an appropriate stiffness matrix was derived. During the implementation of the CVISC constitutive model a mistake related to the plastic dilatancy was detected and reported to ITASCA (proprietary of the commercial finite difference program FLAC), which they later fixed [28].
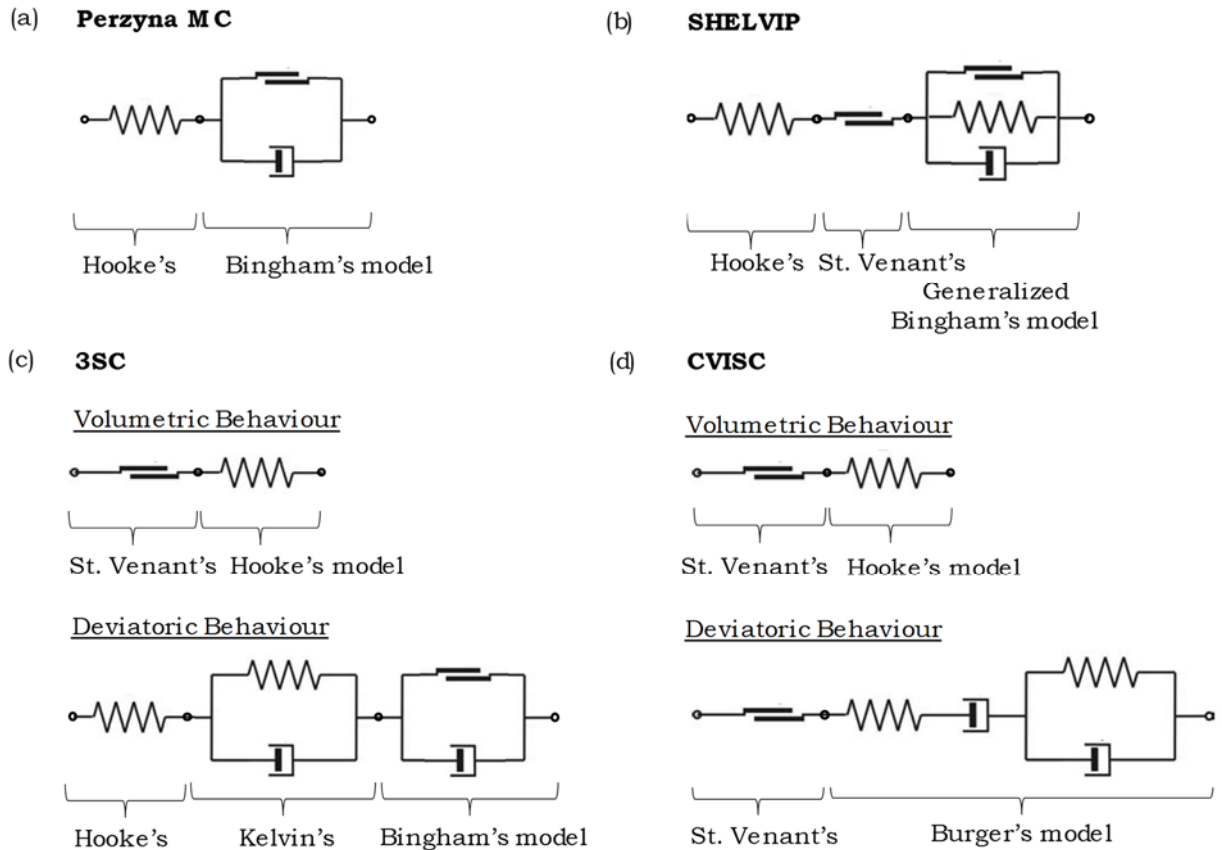
(a) **Perzyna M C**

(b) **SHELVIP**

(c) **3SC**

(d) **CVISC**

Figure 1. Schematic representation of the considered constitutive models

Appendix 2

This Appendix presents and discusses the results of the parametric analysis for evaluating the risks of shield jamming during continuous excavation and standstill and overstressing of the lining of the tunnel in dependency of the constitutive model chosen (*cf.* Section 1.4). The risk of jamming and overstressing is evaluated by comparing the required thrust force of a TBM and the pressure on the lining with typical values of installed thrust force of a TBM and pressure resistance of concrete segments respectively.

Table 1 and 2 show the parameters used in the simulations, Table 3 gives typical values for the lining and for the single shielded TBM (*e.g.* the lining resistance or the installed thrust force) used for comparison with the results of the simulations.

The results are evaluated in terms of the product of viscosity η and advance rate v, because the ground pressure acting on the shield as well as on the lining depend on the overcut but also on the time needed for the ground to close the gap caused by the overcut and the stress redistribution due to deformation. The higher the viscosity, the higher the stress taken immediately by the viscous element. The accumulated stress by the Newton element will be released with time but with a rate invers proportional to its viscosity, *i.e.* the lower the viscosity the faster the release of stress or the higher the deformation rate (time effect of creep). On the other hand, if the advance rate is high enough the shield moves before the ground can develop its full pressure on the shield.

Figure 2 shows the actual normalized ground pressures $p \, / \, \sigma_0$ developing on the TBM shield and lining during excavation calculated with Perzyna MC, CVISC (Kelvin) or CVISC (Maxwell) constitutive models for different products of viscosity and advance rate $\eta \, v$. In general, the results show that the convergences increase with the distance from the face and thus the ground pressures on the shield and lining, however, pressures on the shield will only develop if convergences are bigger than the overcut.

Results calculated with CVISC (Maxwell) for small products $\eta \, v$ (1e3 kPa*m or 1e5 kPa*m) show higher ground pressures next to the tunnel face than at the shield tail (*cf.* Fig. 2c), because of a fundamental characteristic of the constitutive model and of the unsupported face. The constitutive model considers a viscous element in series and therefore ground deformations will only stop when the ground pressures on the shield and lining are equal to the primary stress state. Additionally, an unsupported face leads to higher ground pressures on the shield next to the tunnel face than at the shield tail.

The calculations performed with Perzyna MC and CVISC (Kelvin) model show that pressure developing on the shield increases with the product $\eta \, v$ and reaches a maximum at 5×10^5 and 5×10^6 respectively (*cf.* Figs 2a and 2b). With further increase of the product $\eta \, v$, the pressure on the shield diminishes monotonically. From a product value of 10^9 no substantial change in the pressure can be observed. The described increase and decrease of the pressure on the shield as function of the product $\eta \, v$ is related to the connection of the viscous element in parallel with another rheological element, to the amount of stress and its dissipation rate described above and to the rate of advance. As described above, the initial monotonically increase of the pressure with the product $\eta \, v$ denotes that the stress stored increases and that it can release it partially on the shield until reaching a maximum. With further increase of the product $\eta \, v$ the TBM will move faster or the time for stress dissipation takes longer so that pressure on the shield decreases. This effect is much more pronounced for CVISC (Kelvin) than for Perzyna MC model.

The thrust force F_r required for a restart after a standstill of time t is calculated by integrating the ground pressures p over the shield length at time t:

$$F_r(t) = \mu 2\pi R \int_0^L p(x,t)\,dx \qquad (1)$$

Where μ, R and L denote the shield skin friction coefficient, the radius of the tunnel and the shield length respectively. The thrust force is normalized with respect to the primary total stress σ_0 and the parameters described before:

$$F_r^*(t) = \frac{F_r(t)}{2\pi LR\sigma_0\mu} \qquad (2)$$

Figures 3a to 3c show the normalized required thrust force F_r^* after standstill for different standstill durations, calculated with Perzyna MC, CVISC (Kelvin) or CVISC (Maxwell) constitutive model for different products of η v. To evaluate the risk of jamming also according to Eq. 2 the normalized installed thrust force F_i^* is plotted. In Table 3 the values of the installed thrust force F_i considered in the present study and its normalized value are listed.

With all three considered models, the required thrust force and the ground pressures on the lining show during the initial stage of a standstill an approximately constant and lowest value (*cf.* Figs. 3a to 3c). After the gap is closed, the pressure on the shield will increase following a sigmoid function until reaching new equilibrium and thus achieving steady state. With the Perzyna MC and the CVISC (Kelvin) model an increase of the required thrust force with increasing product of product η v until reaching a maximum can be observed in the beginning of the standstill. Similar as described above for the normalized pressure on the shield during TBM excavation, with further increase of the product η v the required thrust force to restart decreases. With the CVISC (Maxwell) model the required thrust force decreases monotonically with increasing product η v.

The time where pressure on the shield starts to increase is marked in all curves of Figures 3a to 3c and is defined as critical standstill time (t_{crit}). In Figure 4 the critical time over the product η v is plotted in a double-logarithmic scale. In a good approximation, the relation between this critical time and the product of viscosity and advanced rate can be described with a simple function independently of the model adopted. From a practical point of view, this critical time relates to the duration of standstill with the lowest required thrust force to restart and thus it denotes the time available for maintenance without fearing jamming at all. The required thrust force to restart depends strongly on the model adopted and obviously on the viscosity value. The lowest required thrust force is obtained with Perzyna MC and the highest with CVISC (Maxwell). With Perzyna MC there is no risk of jamming at all, *i.e.* for the completely analysed range the required thrust force is smaller than typically installed thrust forces on TBMs even after extremely long standstill times (*cf.* Fig. 3a), while for CVISC (Kelvin) only for low viscous cases and standstill times longer than some days the jamming risk will increase. For long standstill times the required force can exceed twice the typically installed thrust forces on TBMs (*cf.* Fig. 3b). Simulations with CVISC (Maxwell) show even for moderate viscosity and relatively short standstill times a high jamming risk, where the maximal required thrust force can be about three times higher than the typically installed thrust forces on TBMs (*cf.* Fig. 3c).

Figures 5a to 5c show the normalized pressures developing on the lining at a distance of 30 m from the tunnel face (*i.e.* 20 m from the shield tail) over standstill time calculated with Perzyna MC, CVISC (Kelvin) or CVISC (Maxwell) model respectively. The pressure on the lining develops in a similar way as the pressure on the shield described above, *i.e.* during the initial stage of a standstill, an approximately constant and lowest value can be observed. For relatively low

product values of η ν the pressure on the lining is constant, *i.e.* a steady state is reached very fast due to the low viscosity of the ground. With increasing product of η ν results with Perzyna MC and CVISC (Maxwell) model show a monotonically decrease of initial pressure developing on the lining. For CVISC (Kelvin) firstly by increasing the product η ν an increase of the pressure on the lining can be observed. After reaching a maximum further increase of the product of η ν lead to a decrease of the initial pressure on the lining. Similar as described for the required thrust force, with increasing standstill time the pressure on the lining follows a sigmoid function until reaching a constant value (steady state). The latter corresponds to the maximum value and thus it is the relevant pressure value for evaluating the risk of overstressing the lining. Figures 6a to 6c show the normalized maximum pressure on the lining over the product η ν calculated with a Perzyna MC, CVISC (Kelvin) and CVISC (Maxwell) model respectively. Also the normalized adopted lining pressure resistance is plotted in Figure 6. The results with Perzyna MC and CVISC (Maxwell) show approximately constant pressure on the lining (*cf.* Figs. 6a and 6c), *i.e.* there is no dependency of the lining pressure on the viscosity or the advance rate. The curve of the lining pressure calculated with CVISC (Kelvin) model over the product η ν follow a sigmoid function. For the chosen geotechnical conditions, there is a different risk of overstressing of the lining. With Perzyna MC model the calculated pressure corresponds approximately to the typical value of lining strength (safety factor ν = 1). With CVISC model the calculated pressure exceeds the lining strength by factor two and three for CVISC (Kelvin) and CVISC (Maxwell) models respectively making tunnelling in ground behaving like this model extremely problematic if not impossible.

Geotechnical parameter	Symbol	Unit	Value
Young's modulus	E	[GPa]	1
Kelvin's shear modulus	$G^{ve,K}$	[GPa]	0.33[a]
Poisson's ratio	υ	[-]	0.25
Uniaxial compressive strength	f_c	[MPa]	1.5
Angle of internal friction	ϕ	[°]	25
Dilatancy angle	ψ	[°]	5
Unit weight	γ	[kN/m^3]	25
Depth of cover	H	[m]	400
Primary total stress	σ_0	[MPa]	10[b]
Lining			
Young's modulus of the lining	E_c	[GPa]	35[c]
Poisson's ratio of the lining	υ_c	[-]	0.2[c]
Inner radius of the lining	R_{int}	[m]	4.5[d]
Lining thickness	d_l	[cm]	50[e]
Stiffness of the lining	K_l	[MPa/m]	800[f]
Radial gap size	ΔR_l	[cm]	0
TBM			
Boring radius	R	[m]	5[g]
Radial gap size	ΔR	[cm]	5[h]
Length of the shield	L	[m]	10[i]
Young's modulus of the shield	E_s	[GPa]	210
Shield thickness	d_s	[cm]	7.5
Stiffness of the shield	K_s	[MPa/m]	630[j]
Advance rate	υ	[m/d]	1, 10[k]

[a] only for CVISC constitutive model, assumed after [5 - 8] which calibrated this parameter through laboratory test and or field measurements.
[b] $\sigma_0 = \gamma H$.
[c] assumed.
[d] $R_{int} = R - d_l$
[e] minimum thickness for a segmental lining in squeezing ground [9]
[f] calculated under the assumption of a thick walled cylinder [9]
[g] assumed rail tunnel radius.
[h] achieved by changing position of the gauge cutters [29].
[i] assumed.
[j] $K_s = E_s\, d_s\, /\, R^2$.[30]
[k] assumed

Table 1. Geotechnical, segmental lining and TBM parameters adopted for the study of thrust force and lining pressure

Parametric analysis nr.	1	2	3
Constitutive models considered	Perzyna MC	CVISC (Kelvin)	CVISC (Maxwell)
Viscosity parameter [kPa*d]			
$\eta^{ve,M}$ of Maxwell's model	-	∞	10^3-10^{12}
$\eta^{ve,K}$ of Kelvin's model	-	10^3-10^{12}	∞
η^{vp} of Bingham's model	10^3-10^{12}	-	-

Table 2. Constitutive model and viscosity parameters adopted for the study of thrust force and lining pressure

TBM and lining	Symbol	Unit	Value
Concrete compressive strength	$f_{c,l}$	[MPa]	30[a]
Lining strength, p_{max}	p_{max}	[MPa]	3[b]
Installed thrust force	F_i	[MN]	150[c]
Normalized installed thrust force	F_i*	[-]	0.32
Boring force per cutter	F_c	[kN]	267[d]
Number of cutters	n	[-]	67[e]
Thrust force (boring process)	F_b	[MN]	18[f]
Sliding friction coefficient	μ	[-]	0.10[g]
Static friction coefficient	μ	[-]	0.15[g]

[a] assumed.
[b] $p_r = d\,f_{c,l}\,/\,R$ [30].
[c] assumed.
[d] according to [31].
[e] $n = 6.7*2*R$ [32].
[f] $F_b = F_c\,n$.
[g] with lubrication of the shield skin [33].

Table 3. Typical values for the TBM and segmental lining used for comparison with the numerical results
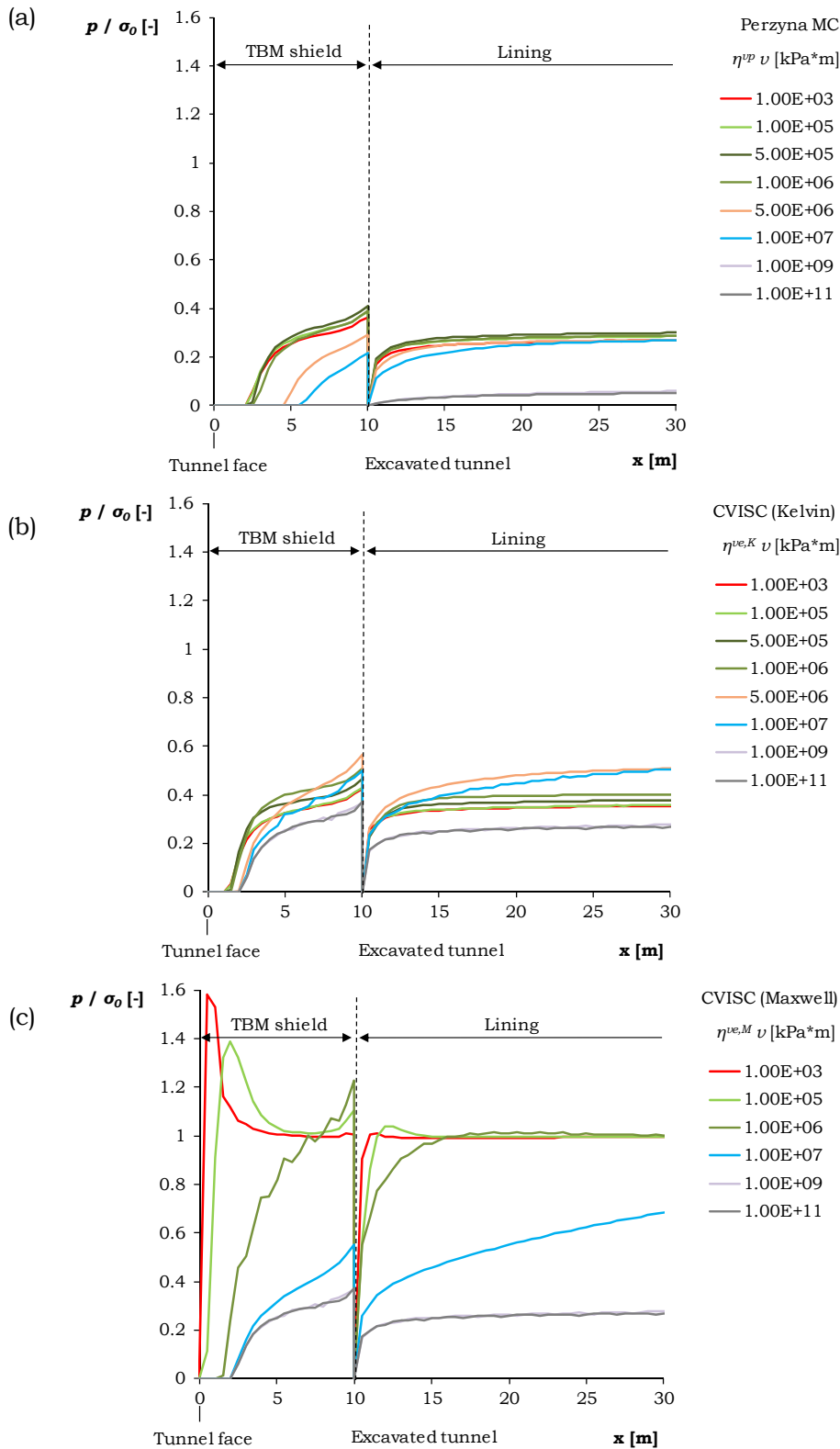
Figure 2. Actual normalized pressure developing over the shield and lining during excavation over current distance from tunnel face calculated with (a) Perzyna MC, (b) CVISC (Kelvin), (c) CVISC (Maxwell) constitutive model
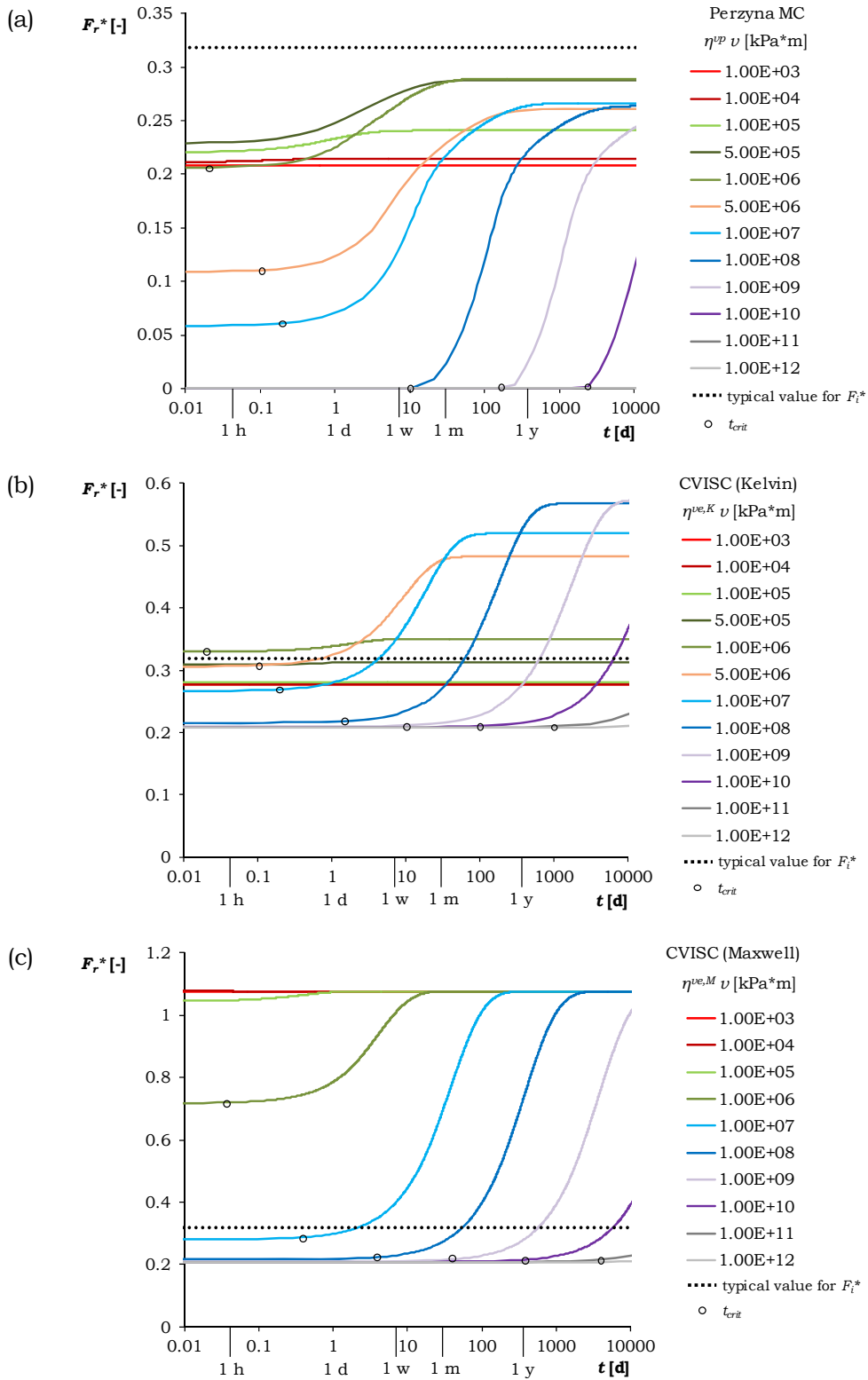
(a)

(b)

(c)

Figure 3. Normalized required thrust force F_r^* for a restart over standstill time calculated with (a) Perzyna MC (b), CVISC (Kelvin), (c) CVISC (Maxwell) constitutive model
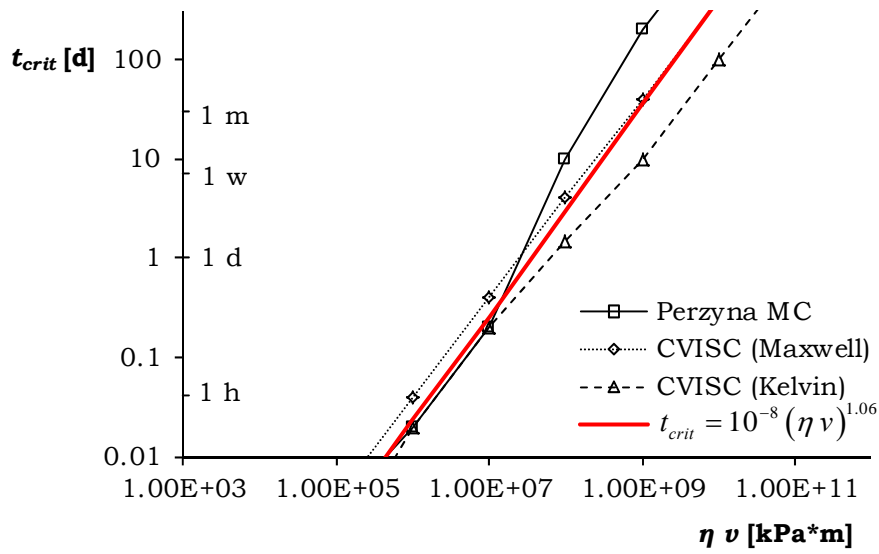
Figure 4. Critical time for standstill over the product $\eta\ v$, calculated with (a) Perzyna MC, (b) CVISC (Kelvin), (c) CVISC (Maxwell) constitutive model
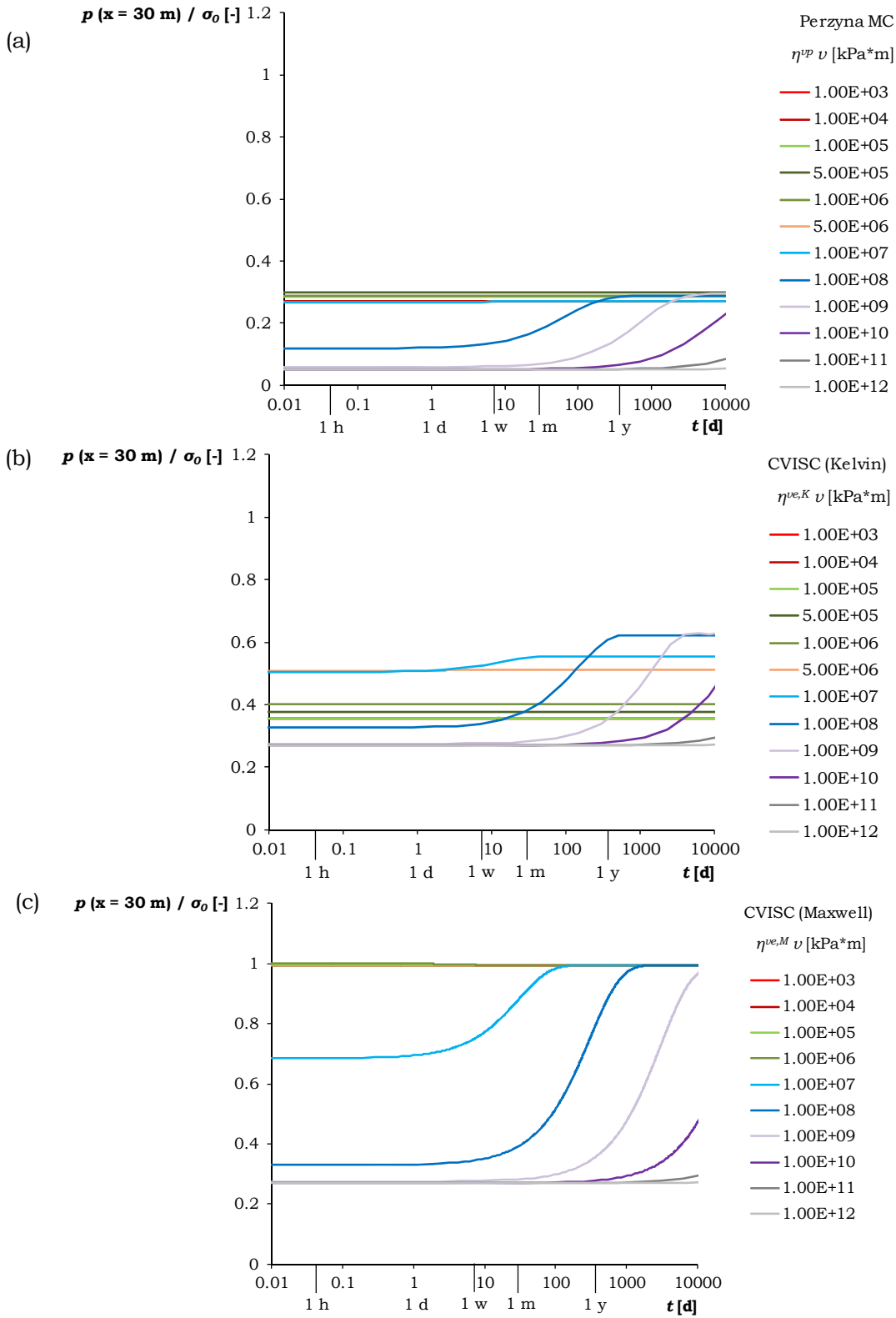
Figure 5. Normalized pressure on the lining developing during standstill at a distance of 30 m from the tunnel face (*i.e.* x = 30 m) calculated with (a) Perzyna MC, (b) CVISC (Kelvin), (c) CVISC (Maxwell) constitutive model
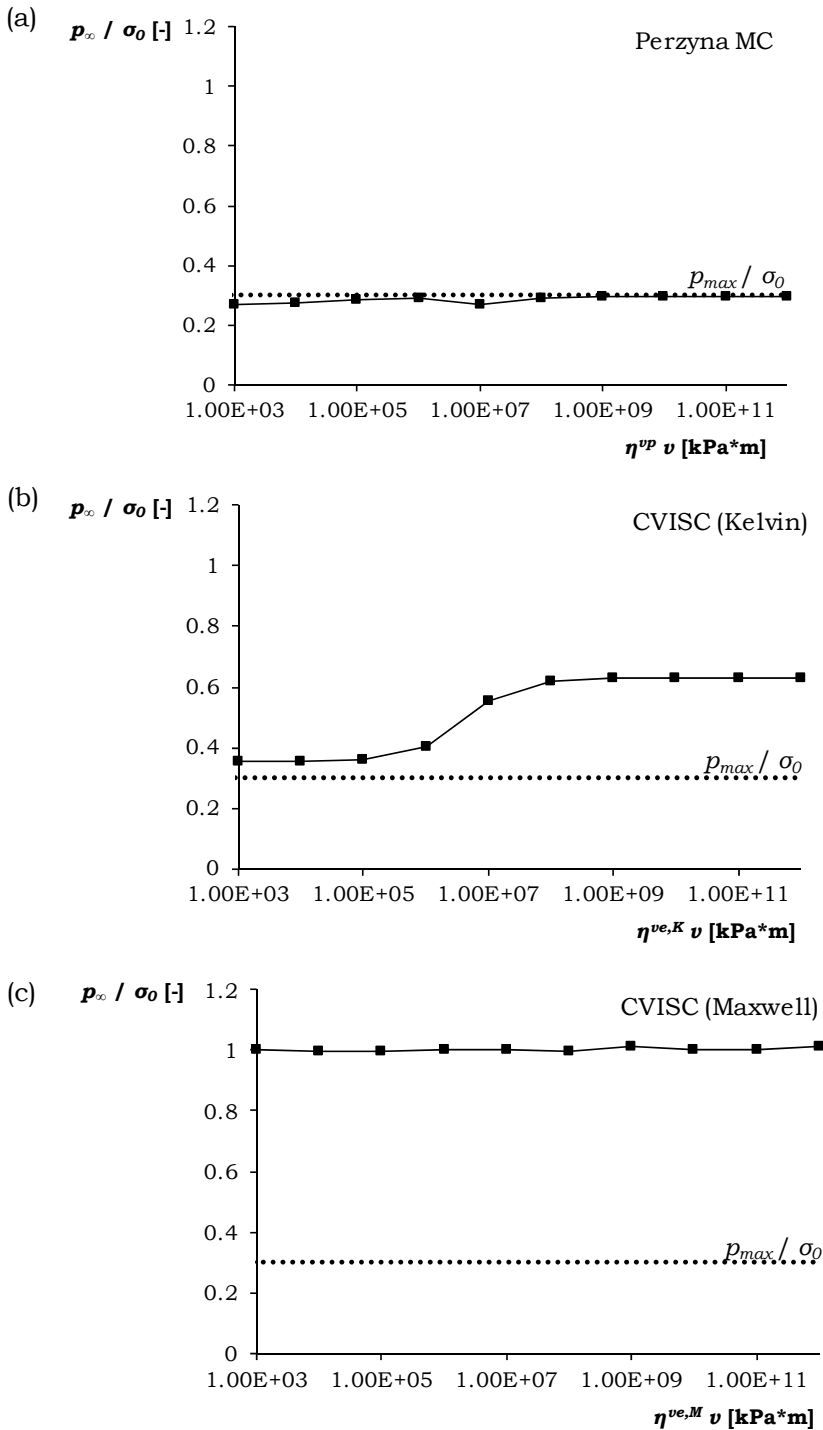
(a)

p_∞ / σ_0 [-]

Perzyna MC

p_{max}/σ_0

$\eta^{vp} v$ [kPa*m]

(b)

p_∞ / σ_0 [-]

CVISC (Kelvin)

p_{max}/σ_0

$\eta^{ve,K} v$ [kPa*m]

(c)

p_∞ / σ_0 [-]

CVISC (Maxwell)

p_{max}/σ_0

$\eta^{ve,M} v$ [kPa*m]

Figure 6. Normalized pressure acting on the lining at steady state function of the product $\eta \, v$ calculated with (a) Perzyna MC, (b) CVISC (Kelvin), (c) CVISC (Maxwell) constitutive model

Appendix 3

This Appendix presents and discusses similarities and differences in the behaviour of a ground either prone to creep or to consolidate. More precisely ground pressures developing on the shield of a TBM during excavation and standstill, the required thrust force to restart tunnelling, the pressure on the lining and the extrusion deformations and stability of the tunnel face are analysed.

The geotechnical and tunnelling parameters for a ground prone to creep are listed in Table 1 of Appendix 2. Table 4 shows the parameters used in the simulations for the case considering only consolidation.

Analogous to the risk study of shield jamming the results of the creep case are evaluated in terms of the product of viscosity η and advance rate v (*cf.* Appendix 2). For the consolidation case the evaluation is done in terms of the ratio of advance rate v to ground permeability k.

Figures 7 to 9 show the results calculated considering either only creep or consolidation of the actual normalized ground pressures p / σ_0 developing on the TBM shield and lining during excavation, of the normalized required thrust force F_r^* after standstill of different standstill durations and of the normalized pressures developing on the lining at a distance of 30 m from the tunnel face (*i.e.* 20 m from the shield tail) over standstill time. Although the Figure on the top of each of these Figures is identical with the corresponding Figures 2, 3 and 5 in Appendix 2 they are plotted here again in order to facilitate the direct comparison of the results between the creep and the consolidation case. Thus as far as results of both cases show similar curves the same observations described in Appendix 2 apply here. Similar behaviour concerning the ground pressure developing in the TBM and lining, the required thrust force to restart tunnelling after standstill and the pressure on the lining can be observed in both cases (creep and consolidation). That applies to the shape of the curves, to maximal and minimal values and to the variability of the parameters, which differs by three order of magnitudes, *i.e.* approximately the same results are obtained if $\eta\ v\ 10^3 = v\ /\ k$.

Geotechnical parameter	Symbol	Unit	Value
Permeability	k	[m/s]	10^{-6}-10^{-15}
Compressibility of the grains	c_g	[1/MPa]	0
Compressibility of the water	c_w	[1/MPa]	0
Initial hydraulic head	h_0	[m]	100
Unit weight of water	γ_w	[kPa/m³]	10
Primary effective stress state	σ'_0	[MPa]	9[a]

a $\sigma'_0 = \gamma\ H - \gamma_w\ h_0$.

Table 4. Geotechnical parameters for a ground prone to consolidate adopted for the study of qualitatively comparison between consolidation and creep mechanisms
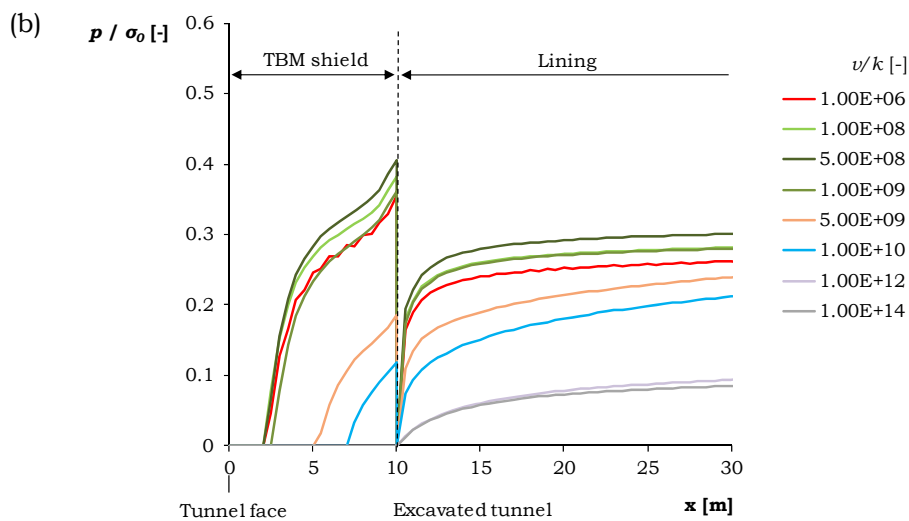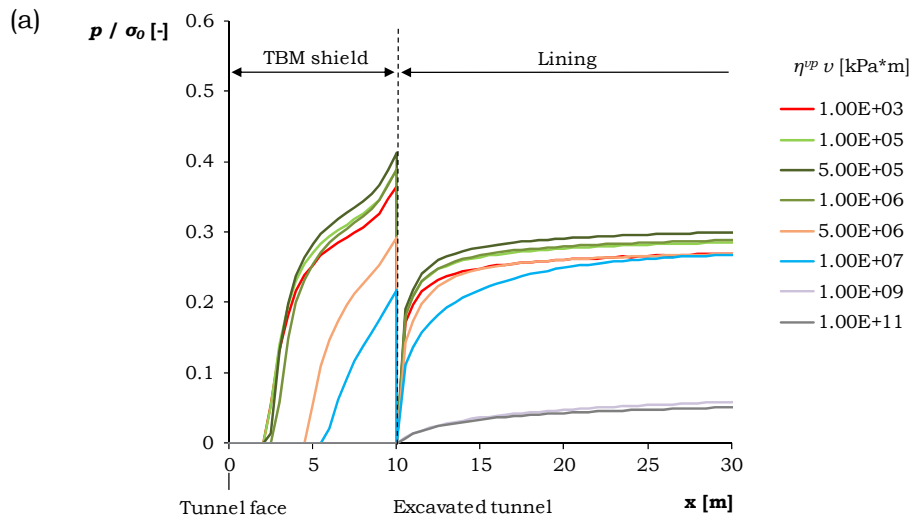
(a)

(b)

Figure 7. Actual normalized pressure developing over the shield and lining during excavation over current distance from tunnel face calculated considering only (a) creep, (b) consolidation mechanism
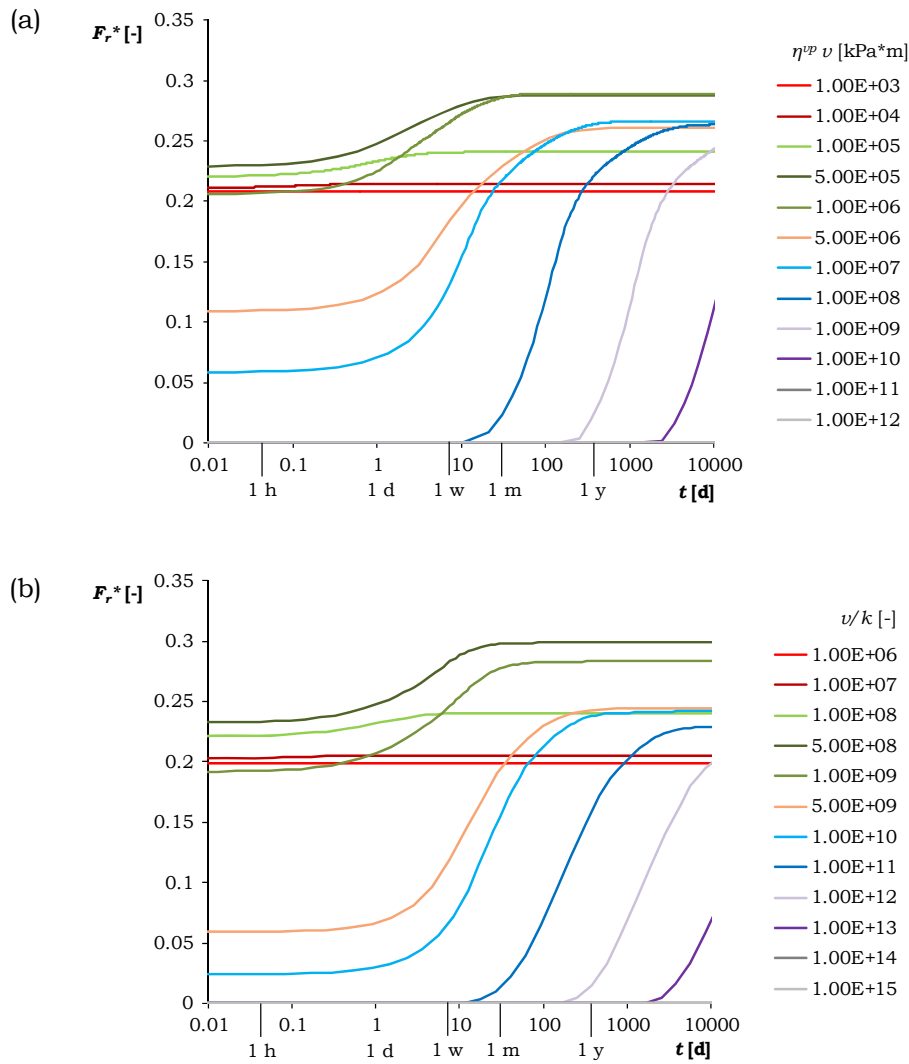
Figure 8. Normalized required thrust force F_r^* for a restart over standstill time calculated considering only (a) creep, (b) consolidation mechanism
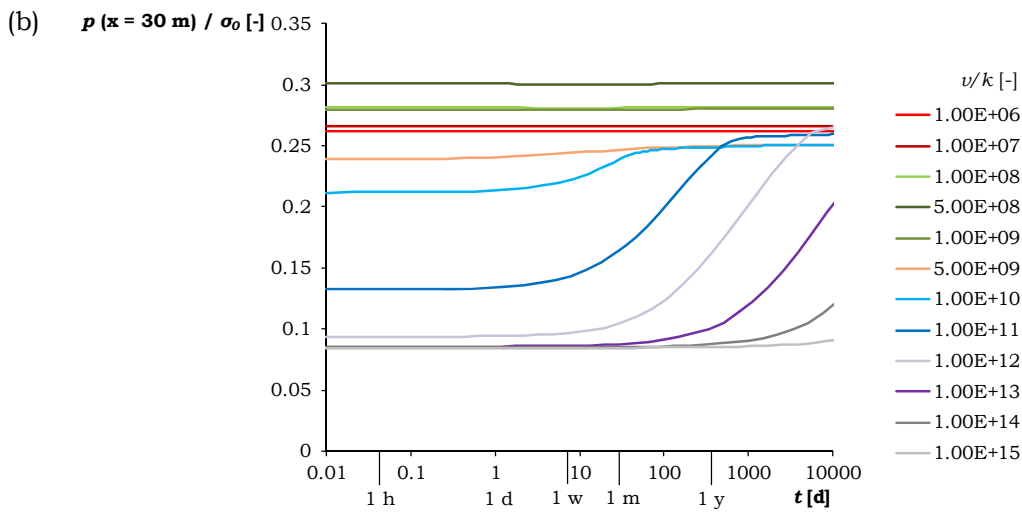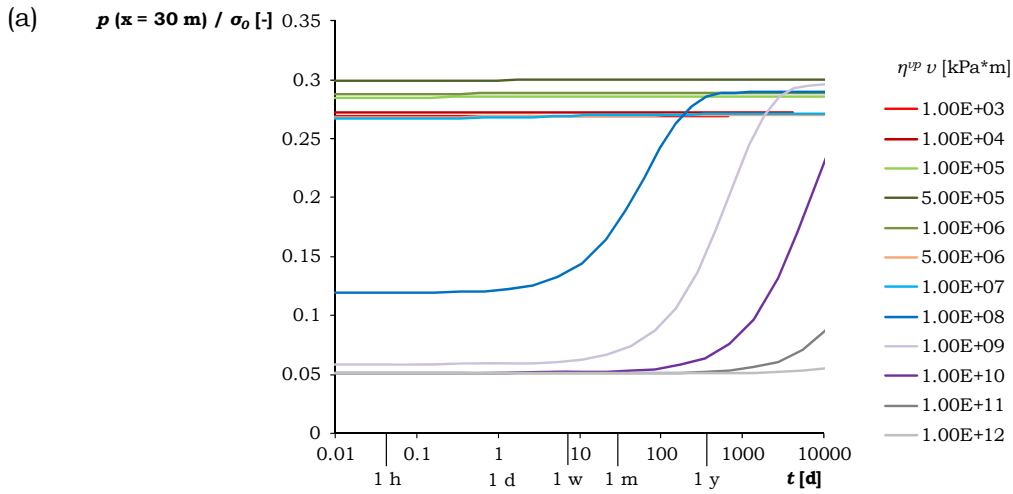
(a)

p (x = 30 m) / σ_0 [-]

(b)

p (x = 30 m) / σ_0 [-]

Figure 9. Normalized pressure on the lining developing during standstill at a distance of 30 m from the tunnel face (*i.e.* x = 30 m) calculated considering only (a) creep, (b) consolidation mechanism